Magnetic response of magnetic ion-doped nanocrystals: Effects of single Mn^{2+} impurity

Shun-Jen Cheng
Department of Electrophysics, National Chiao Tung University, Hsinchu 300, Taiwan, Republic of China
(Received 23 August 2005; revised manuscript received 24 October 2005; published 29 December 2005)

We theoretically study the effects of single spin-5/2 magnetic impurity (Mn^{2+}) on the magnetic response of nanocrystals containing interacting electrons. The energy spectrum and magnetic susceptibility of II-VI spherical nanocrystals as a function of the electron number ($N_e=1-8$) and the location of Mn^{2+} ion are calculated by using the configuration interaction method. It is found that the *sp-d* coupling between the carriers and Mn^{2+} ion significantly affects the low-field paramagnetism, depending on electron number and the location of the ion. The competition between electron-electron interaction and the *sp-d* coupling leads to the pronounced anisotropy of magnetic properties, ground state transitions in magnetic field, and the violation of Hund's second rule.

DOI: 10.1103/PhysRevB.72.235332 PACS number(s): 68.65.Hb, 75.20.−g, 75.75.+a

I. INTRODUCTION

Magnetic ion-doped nanostructures have recently drawn a great deal of interest because of the potential application in spin electronics and quantum information technology. Advances in the technology of material synthesis and fabrication have made it possible to incorporate a controlled number of magnetic ions (typically Mn^{2+}) into individual colloidal nanocrystals (NCs)[1–4] or self-assembled quantum dots (SQDs).[5,6] Spin devices based on such semimagnetic nanostructures have also been proposed for detecting or manipulating individual spins in quantum computing.[7,8] Recently, optical emission spectra from single magnetic ion-doped SQDs have revealed the zero-field spin splitting of exciton-Mn hybridized states, created by the *sp-d* coupling between exciton and Mn^{2+} ion.[5] It is known that the *sp-d* coupling is associated with a series of fascinating physical phenomena,[9] e.g., the carrier-mediated ferromagnetism,[10–12] giant Zeeman splitting,[13] and exciton magnetic polaron.[14,15] It also plays a crucial role in the development of spin devices based on semimagnetic nanostructures.

Besides the need for the studies of electron-hole properties,[16–19] there exists also current necessity to explore the properties of magnetic ion-doped nanostructures with only one type of carrier (electrons or valence holes) toward the realization of *spinelectronics*. While the electrical properties of individual nonmagnetic nanostructures[20–28] and Mn-ion doped bulk semiconductors[10] have been extensively studied both experimentally and theoretically, relevant studies of magnetic ion-doped nanostructures are still limited.[29–31] In this paper, we present theoretical results on the magnetic response of the interacting II-VI NCs with few electrons and a single Mn^{2+} ion. We will show that the measurement of magnetic response provides a way to understand the ground state properties of the semimagnetic nanostructures. These theoretical studies are particularly timely because the newly developed techniques of doping and single-nanocrystal spectroscopy have shown the feasibility to synthesize and probe individual NCs with tunable charge.[1,21,32,33]

This paper is organized as follows. In Sec. II, we introduce the model Hamiltonian for an interacting spherical NC with few electrons and a single Mn^{2+} ion, and describe the theoretical methods for the calculation of the electrical and magnetic properties. In Sec. III, we present the numerical results on the energy spectra and the magnetic susceptibility of NCs as a function of electron number and the location of Mn^{2+}, and discuss the effects of dot size and temperature on the magnetic response of a NC. We conclude in Sec. IV.

II. THE MODEL HAMILTONIAN

We model the confinement potential of a nanocrystal quantum dot using the hard wall spherical model.[34] In the framework of the effective mass approximation, the eigenenergy of a single electron in a semiconductor NC at zero magnetic field is explicitly given by $\epsilon_{nl}=(\hbar^2\alpha_{nl}^2)/(2m^*a^2)$. The electron wave function of the corresponding state is $\phi_{nlm\sigma}(\vec{r})=\sqrt{2/a^3}[J_l(\alpha_{nl}/ar)/J_{l+1}(\alpha_{nl})]Y_{lm}(\theta,\phi)$, where a denotes the dot radius, $m^*=0.15m_0$ the effective mass of electron in CdSe, n the principal quantum number, l the angular momentum, m the z-component of angular momentum, $\sigma=\uparrow/\downarrow$ the spin of electron, $J_l(r)$ the spherical Bessel function, α_{nl} the nth zero of J_l, and $Y_{lm}(\theta,\phi)$ the spherical Harmonic function.[34,35]

The Hamiltonian of the interacting few-electron NC doped with single Mn^{2+} subject to magnetic field $\vec{B}\|\vec{z}$ is written as

$$H=T+H_Z+H_{ee}+H_{e\text{-Mn}}. \tag{1}$$

Here the single-particle kinetic energy T is given by

$$T=\sum_{i\sigma}\epsilon_i c_{i\sigma}^+c_{i\sigma}+\sum_{i\sigma}\mu_B^*Bm_ic_{i\sigma}^+c_{i\sigma}+\sum_{ij\sigma}\frac{e^2B^2a^2}{8m^*}D_{ij}c_{i\sigma}^+c_{j\sigma}, \tag{2}$$

where $c_{i\sigma}^+$ ($c_{i\sigma}$) is the creation (annihilation) operator for the electron in the state $|i;\sigma\rangle=|n_i,l_i,m_i,\sigma\rangle$, $\mu_B^*=\hbar e/(2m^*)$ is the effective Bohr magneton, and the matrix element D_{ij} is defined as $D_{ij}\equiv\langle i|(x^2+y^2)/a^2|j\rangle$. The second term in Eq. (2), linear in B and referred to as the orbital Zeeman term, arises from the coupling between the orbital motion of charged particle and applied magnetic field. It contributes (Curie)

paramagnetism to magnetic response of dot. In contrast, the last B-quadratic term contributes (Langevin) diamagnetism. For a small dot in weak magnetic field [$l_B \gg a$, where $l_B = \sqrt{\hbar/(eB)}$ is the magnetic length], the diamagnetism term is negligible but the paramagnetism from the orbital Zeeman terms might make a significant contribution to the magnetic response of dot.

The spin Zeeman term is given by $H_Z = \mu_B^*(m^*/m_0)B(g_e\Sigma_{i\sigma}\sigma_z c_{i,\sigma}^+ c_{i,\sigma} + g_M I_z)$, where $\sigma_z = +1/2(-1/2)$ denotes the z-component of spin up (down) of electron, I_z the z-component of spin of Mn^{2+}, $g_e=1.2$ the g-factor of electron in CdSe NC, and $g_M=2.0$ the g-factor of Mn^{2+}. The effect of the spin Zeeman terms is weak, compared with that of the orbital Zeeman terms, because of the small value of the electron effective mass ($m^*/m_0 \ll 1$).

The particle-particle interaction is given by $H_{ee} = \frac{1}{2}\Sigma_{ijkl}\Sigma_{\sigma\sigma'} V_{ijkl}^{ee} c_{i\sigma}^+ c_{j\sigma'}^+ c_{k\sigma'} c_{l\sigma}$ with the Coulomb matrix element defined as $V_{ijkl}^{ee} \equiv \int\int d^3r_1 d^3r_2 \phi_i^*(\vec{r}_1)\phi_j^*(\vec{r}_2)(e^2/4\pi\kappa|\vec{r}_1 - \vec{r}_2|)\phi_k(\vec{r}_2)\phi_l(\vec{r}_1)$, where $\kappa = 8.9\epsilon_0$ is the dielectric constant of CdSe.[35] The Coulomb matrix elements are evaluated following the approach described in Ref. 34.

The sp-d coupling between electron-Mn^{2+} reads[12,35]

$$H_{e\text{-Mn}} = \sum_{i,\sigma}\sum_{i',\sigma'} J_{ii'}(\vec{s}_{\sigma\sigma'}\cdot\vec{I})c_{i\sigma}^+ c_{i'\sigma'}, \tag{3}$$

with the coupling constant given by

$$J_{ii'} = -[\alpha F_i^*(\vec{R}_I)F_{i'}(\vec{R}_I)]a^{-3}, \tag{4}$$

where $\vec{R}_I$ denotes the position of the Mn^{2+} ion, the function F_i is defined as the dot-size independent part of the single-particle wave function, i.e., $\phi_{nlm}(\vec{r}) \equiv (1/\sqrt{a^3})F_{nlm}(\vec{r})$, and the e-Mn^{2+} exchange parameter $\alpha N_0 = 0.26$ eV is taken for Mn^{2+} impurity in CdSe, where N_0 is the number of cation in unit volume of crystal.[9,35] Here we neglect the electrostatic potential provided by Mn ions and characterize the magnetic ion with its spin alone. This is based on the fact that, unlike the Mn ions acting as acceptors and binding holes in III-V materials,[10,20] Mn ions in II-VI compounds are divalent and neither introduce nor bind carriers.[10,12] The approximation has been widely adopted in previous studies of Mn-doped II-VI semiconductors.[12,16,30,31] Obviously, the sp-d coupling causes spin flips and the electron transferring between orbital states. The former (latter) action violates the conservation of the total spin (the total angular momentum) of electrons. The minus sign in Eq. (4) indicates that a carrier gains energy from the spin-exchange interaction if its spin is aligned with that of Mn ions. The expression of Eq. (4) also indicates that the strength of the sp-d coupling is significantly increased if the dot radius a is very small.

The electron-Mn^{2+} configurations can be classified by the total number of electron N_e, the z-component of the total angular momentum L_z, the z-component of total electron spin S_z, and the z-component of Mn^{2+} spin I_z. In this paper, we consider the NCs with electrons ($N_e=1-8$) filling the two lowest electronic shells, the s-shell state ($n=1$, $l=0$, $m=0$) and the p-shell states ($n=1$, $l=1,m$), consisting of the p^- ($m=-1$), the p^0 ($m=0$), and the p^+ ($m=+1$) states. Figures 1(a) and 1(b) show the E-m diagram of the s and p states and the corresponding wave functions in real three-dimensional (3D) space, respectively. For strongly quantized small NCs, particle scattering to higher shells is negligible and we can build up the configurations $|N_e, L_z, S_z; I_z\rangle$ in the two-shell (the s- and p-shells) approximation. In the basis of the configurations, we expand the wave function of few-particle states, diagonalize the corresponding Hamiltonian matrix, and calculate the eigenstates and energies $\{E_i\}$.[36,37]

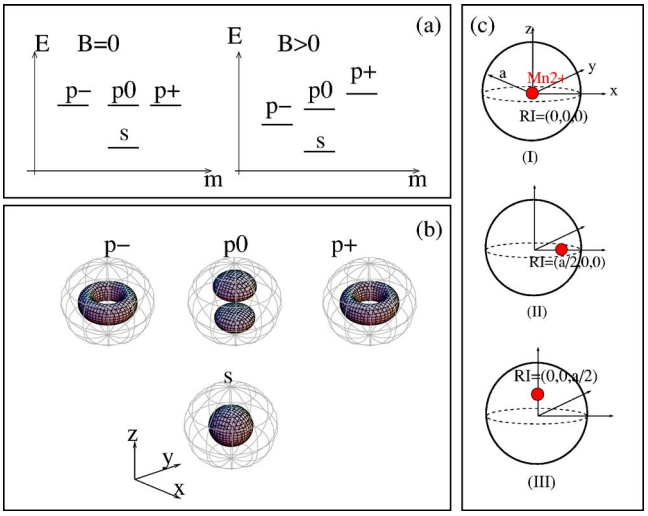

FIG. 1. (Color online) (a) Schematic E-m diagram of spherical nanocrystal (NC) at zero and finite magnetic fields. (b) Isosurfaces of the electron densities of the s- and p-states of NC. (c) Schematic illustration of the three case studies of the location of Mn ion in NC in this paper.

The magnetization of N_e-electron dot at temperature T is given by $M = k_B T(\partial \ln Z/\partial B)_T$, where $Z = \Sigma_i \exp[-E_i(N_e;B)/(k_B T)]$ is the canonical ensemble equilibrium partition function and k_B the Boltzmann constant. The magnetic susceptibility, defined as $\chi \equiv \partial M/\partial B$, is calculated by standard three-point numerical derivation.[25–28]

III. RESULTS AND DISCUSSIONS

A. Magnetic susceptibility as a function of electron number and Mn^{2+} position

To explore the effect of electron number and position of Mn, we study a CdSe NC with single Mn^{2+} impurity and electron number $N_e=1-8$ in three representative cases of the Mn^{2+}-ion position, i.e., $R_I=(0,0,0)$, $R_I=(a/2,0,0)$, and $R_I=(0,0,a/2)$ [see Fig. 1(c)].

1. Dots with filled s-shell

First, we consider the simplest case: the NC quantum dot containing a single electron and a single magnetic ion at the dot center. In the absence of the sp-d coupling, the combination of the electron with $S_z=1/2$ or $-1/2$ and the magnetic ion ($I=5/2$) with six possible spins $I_z=\pm 1/2, \pm 3/2, \pm 5/2$ yields the 12-fold degenerate ground states (GSs) at zero magnetic field. Turning on the coupling to Mn, the zero-field degeneracy is lifted and splits into two groups, correspond-

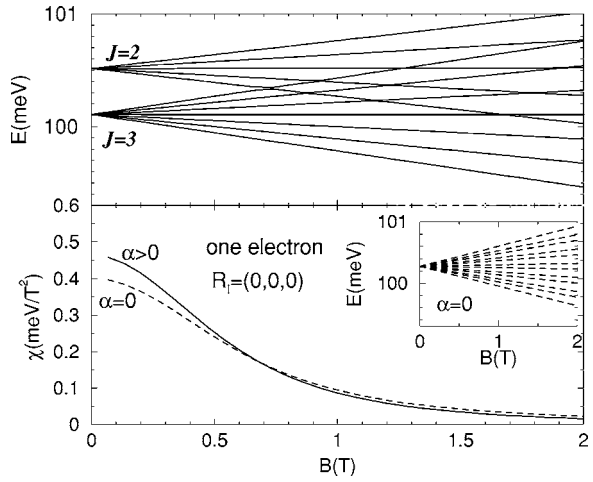

FIG. 2. (a) Calculated low-lying energy spectrum of CdSe NC, $a=5$ nm in radius, with $N_e=1$ and single Mn^{2+} ion located at the dot center in magnetic field B. (b) Calculated magnetic susceptibility χ of the NC vs magnetic field. The dashed line corresponds to the result calculated without the consideration of the *sp-d* coupling ($\alpha=0$). The inset shows the energy spectrum calculated with $\alpha=0$.

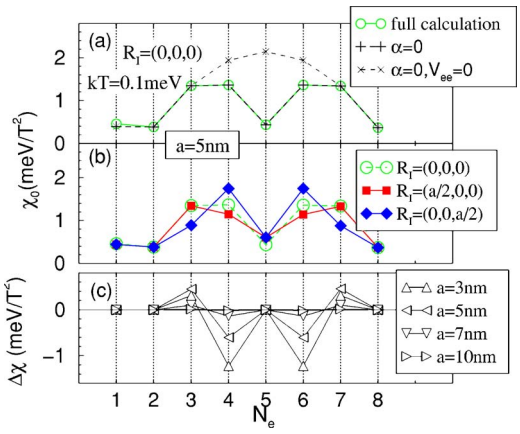

FIG. 3. (Color online) Calculated zero-field magnetic susceptibility as function of electron number. (a) Circles show the result of full calculation for Mn located at dot center. Symbol + (×) labels the result calculated without the inclusion of the *sp-d* coupling (the *sp-d* coupling and Coulomb interaction). (b) Filled squares (diamonds) show the result of full calculation for Mn located at $R_I=(a/2,0,0)$ [$R_I=(0,0,a/2)$]. (c) The anisotropy quantity $\Delta\chi$ (see text) is shown as a function of electron number N_e and the dot radius a.

ing to the two possible total angular momenta of electron and Mn^{2+} ion complex, $J=2$ and 3 ($\vec{J}\equiv\vec{S}+\vec{I}$). Figure 2(a) shows the calculated energy spectrum versus magnetic field of the NC with radius $a=5$ nm. For comparison, the energy spectrum calculated without the inclusion of the *sp-d* coupling ($\alpha=0$) is shown in the inset in Fig. 2. The *sp-d* coupling is found to lower the energy of the *e*-Mn GS by only a few tens of μeV.

Figure 2(b) shows the magnetic susceptibility of the single-electron NC as a function of B at the low temperature $k_BT=0.1$ meV, calculated with and without the inclusion of the *sp-d* coupling. We see that, with the $\vec{S}\cdot\vec{I}$ coupling, the magnetic susceptibility slightly increases at low field $B\to 0$. In the Curie law, the magnetic susceptibility from a particle with angular momentum $J=I+S$ in the limit $B/T\to 0$ follows the equation

$$\chi_J=\frac{\mu_{eff}^2}{3k_B}\frac{1}{T}, \tag{5}$$

where μ_{eff} denotes the effective moment given by $\mu_{eff}=g_J\mu_B\sqrt{J(J+1)}$, where μ_B is the bare Bohr magneton and g_J the Lande g-value.[38] Accordingly, it can be shown that the paramagnetism from a single particle with $J=3$, created by the $\vec{S}\cdot\vec{I}$ coupling, is higher than that from a system with decoupled $S=1/2$ electron and $I=5/2$ Mn, i.e., $\chi_J>\chi_I+\chi_s$.[39] However, the increase of the low-field magnetic susceptibility $\chi(B\to 0)$ is small and turns out to be negligible as temperature is further raised or the magnetic ion is moved away from the dot center. In this one-electron case, the effect of the *sp-d* coupling on the magnetic response of the dot is found to be very weak.

For $N_e=2$ dot, the terms of the orbital Zeeman, spin Zeeman, and the *sp-d* coupling vanish because of the zero total angular momentum and the zero total spin of the GS. The dot exhibits a similar feature of paramagnetism vs B to that shown in Fig. 2(b), but the paramagnetism is completely originated from the Mn^{2+} ion.

2. Dots with filled s- and p-shells

For $N_e\geqslant 3$, electrons start to populate the p-shell states ($l=1$). There are two notable features. (1) The paramagnetism of the dot with filled p-shell is significantly increased because total angular momentum becomes finite. (2) A Mn^{2+} ion in dot is coupled to certain p-orbital states, depending on its position, and the orbital states coupled to the Mn^{2+} impurity are favorable for electron (at low field) prior to fill for gaining spin-exchange energy. The first feature has been extensively studied for atoms[38] and nonmagnetic quantum dots.[40–42] Figure 3(a) shows the calculated zero-field magnetic susceptibility $\chi_0=\chi(B\to 0)$ as a function of electron number of the dots with a single Mn^{2+} impurity at the dot center for the low temperature $k_BT=0.1$ meV. In this case, the *sp-d* coupling actually has no effect on the magnetic response because the Mn ion resides at the node of the p-shell wave functions. We see that the magnetic susceptibility is significantly increased for $N_e\geqslant 3$, except for $N_e=5$ ($N_e=8$) where the p-shell is half (completely) filled. For $N_e=5$ and 8, the GSs have zero orbital angular momentum $L=0$ following Hund's rules, and the magnetic susceptibilities are minimized. The pattern of the plot of χ_0 versus N_e is analogous to that of orbital angular momentum versus electron number, L vs N_e, and can be treated as the manifestation of the GS properties.

The second feature, existing only in magnetic ion-doped dot, might drastically affect the *e*-Mn GS and even violate the underlying principle of dots, like Hund's rules. Unlike the cases of $N_e=1,2$, the effects of the *sp-d* coupling on the NCs with filled p-shell cause not only the flip of particle spin

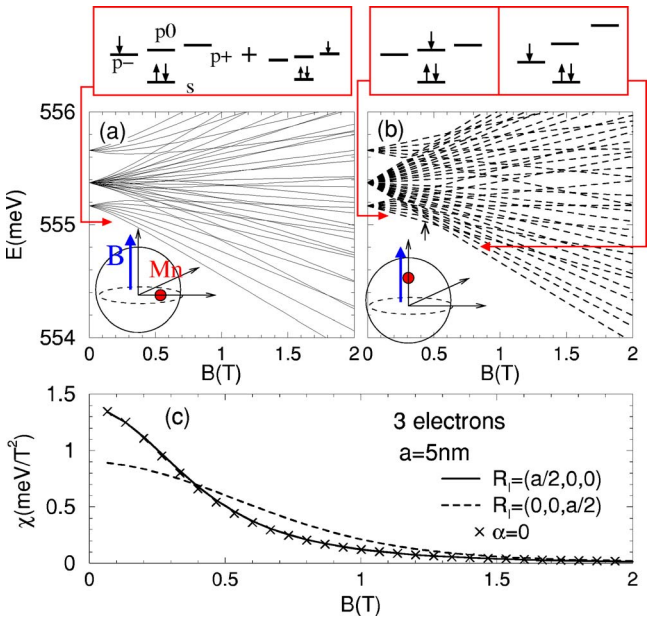

FIG. 4. (Color online) Calculated energy spectrum of the CdSe NC with $N_e=3$ and a single Mn^{2+} ion located at (a) $\vec{R}_I=(a/2,0,0)$ and (b) $\vec{R}_I=(0,0,a/2)$. (c) Solid and dashed lines show the corresponding magnetic susceptibilities. Symbol × denotes the result calculated with $\alpha=0$.

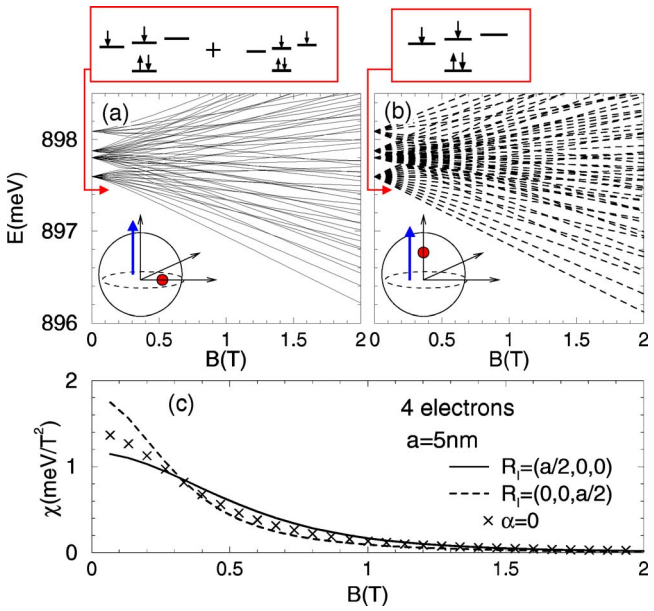

FIG. 5. (Color online) The same as Fig. 4, but for the four-electron dot.

but also the transferring of particles between different orbital states. In finite fields, the latter effect competes with the orbital Zeeman term, which favors the electron to stay in the state with the lowest angular momentum, and gives rise to abrupt GS transitions for some cases of electron number. We will see how such GS transitions directly impact the magnetic properties of NCs.

Figures 4(a) and 4(b) show the energy spectrum versus B of $N_e=3$ NC with the Mn^{2+} ion located at $R_I=(a/2,0,0)$ and $R_I=(0,0,a/2)$, respectively. There are six configurations involved in the GSs, $c^+_{i,\sigma}c^+_{s\downarrow}c^+_{s\uparrow}|0\rangle$, where $i=p^+,p^0,p^-$ and $\sigma=\uparrow/\downarrow$. In the presence of Mn^{2+}, two of them are subject to the *sp-d* coupling while the other four are not. Thus the states involving the two Mn^{2+}-coupled configurations are split into two groups with $J=2$ and 3. The other states decoupled from Mn^{2+} stay at their original levels. Hence we see three level groups appearing in the spectra of Figs. 4(a) and 4(b).

In the former case, the Mn ion at $R_I=(a/2,0,0)$ is coupled to both p^+ and p^- orbital states. The Mn^{2+} ion as an impurity in dot causes backscattering and reverses the moving direction of the particle with some finite angular momentum. Thus, via the coupling, particle transferring between the two orbital states with opposite angular momentum is possible. The GS of the $N_e=3$ NC with the Mn^{2+} ion turns out to be the intermixture of the configuration with $L_z=-1$, $c^+_{p^-\downarrow}c^+_{s\downarrow}c^+_{s\uparrow}|0\rangle$ and that one with $L_z=+1$, $c^+_{p^+\downarrow}c^+_{s\downarrow}c^+_{s\uparrow}|0\rangle$. The intermixing of the configurations, indicating the break of conservation of total angular momentum, weakens the B-dependence of the GS level and suppresses the magnetic susceptibility at small fields [see Figs. 4(a) and 4(c)]. The *quenching* of the orbital angular momentum occurs, however, only at extremely weak field ($L_z\sim 0$ as $B\sim 0$) for the large dot with $a=5$ nm. The reduction of the magnetic susceptibility becomes more obvious if the dot size is reduced to $a\lesssim 3$ nm.

If the Mn^{2+} ion is moved to the z-axis position $R_I=(0,0,a/2)$, the ion is coupled to the p^0 states alone. In this case, L_z is still a good quantum number and no particle transferring happens. At small fields ($B<0.6$ T), the topmost electron in the GS stays in the p^0 state for gaining spin-exchange energy and the total angular momentum is zero. Increasing B, the increasing orbital Zeeman energy lowers the energy level of the p^- state. At the critical field $B\sim 0.6$ T, the Zeeman energy overwhelms the strength of the *sp-d* coupling and drives the electron in the p^0-state to the lower p^--state. Thus the $N_e=3$ NC undergoes a abrupt GS transition in magnetic field, as shown in Fig. 4(b). The zero orbital angular momentum of the GS at the small fields leads to extremely low magnetic susceptibility [see Fig. 4(c)]. As a result, the magnetic response of the dot with filled p-shell to low field exhibits pronounced anisotropy with respect to the position of the Mn^{2+} ion [see Fig. 4(c)]. Figure 3(c) shows the quantity of magnetism anisotropy $\Delta\chi$, defined by the difference of $\Delta\chi\equiv\chi_0[\vec{R}_I=(a/2,0,0)]-\chi_0[(0,0,a/2)]$, as a function of electron number and dot radius. We see that the anisotropy of magnetic response strongly depends on electron number and increases with decreasing the size of NC. We note that the $N_e=3$ GSs of the prementioned NCs with a Mn ion located apart from the dot center have $L_z\to 0$ as $B\to 0$. In these cases, Hund's second rule is found to be violated.[43]

For $N_e=4$ dots, the anisotropy still exists but, interestingly, shows the opposite relationship to the position of magnetic ion. Figures 5(a) and 5(b) show the energy spectrum of the $N_e=4$ NCs with the Mn^{2+} ions located at $R_I=(a/2,0,0)$ and $R_I=(0,0,a/2)$, respectively. In contrast to the case of $N_e=3$, the low-field magnetic susceptibility is decreased as

the Mn^{2+} ion is located at the x axis, as shown in Fig. 5(c). In this case, an electron in the $N_e=4$ GS could occupy either p^+ or p^- states, both of which are coupled to the Mn^{2+} ion. The two dominant configurations with opposite total angular momenta ($L_z=+1$ and -1), schematically depicted in Fig. 5(a), are highly intermixed in the GS at small B via the particle transferring between the $p+$ and $p-$ orbitals due to impurity scattering. In the absence of impurity at the x axis, the particle transferring cannot occur (L_z is conserved) and the two configurations shown in Fig. 5(a) are decoupled. The GS level turns out to be a little sensitive to B and magnetic susceptibility is reduced in weak magnetic field. As the Mn^{2+} ion is located at the z axis, the two topmost electrons in the GS, respectively, occupy the p^0 and p^- states, and form a spin-triplet ($S=1$) state to gain both electron-electron and electron-Mn exchange energies. Like the case of $N_e=1$, the magnetic susceptibility is increased due to the spin-spin coupling between the Mn^{2+} ($I=5/2$) and the sole main configuration ($S=1$). In Figs. 5(a) and 5(b), we see that the GSs of both $N_e=4$ Mn-doped NCs are spin-triplet, consistent with the results given by Hund's first rule. However, Hund's second rule is violated again for the $N_e=4$ NC doped with the Mn at the x axis because its GS has $L_z\rightarrow 0$ ($|L_z|\neq 1$) as $B\rightarrow 0$.[43]

According to Hund's rules, the GSs of the $N_e=5$ undoped dot are those spin-fully polarized states with $S=3/2$ and $L_z=0$, in which the three topmost electrons have the same aligned spin and each of them singly occupies one of the p-states. The zero angular momentum of the GS leads to very weak paramagnetism [see Fig. 3(b)]. In the presence of Mn^{2+}, the ion is coupled to all of the $S=3/2$ electron configurations because all p-orbital states are filled with electrons, and the GSs split into four groups corresponding to $J=1$, 2, 3, and 4. Similar to the case of $N_e=1$ (both are the dot with the half filled shell), the sp-d coupling yields the GS with $J=S+I=4$, and the magnetic susceptibility is slightly increased at low field.

The magnetic response of the $N_e=6$ dot is similar to that of the $N_e=4$ dot. The result can be straightforwardly understood by simply treating the empty states on the p-shell as hole with opposite spin. The same symmetry exists also for $N_e=3$ and $N_e=7$ ($N_e=2$ and $N_e=8$). Comparing Figs. 3(a) and 3(b), the low-field paramagnetism χ_0 of the dot is significantly affected by the Mn^{2+}, and strongly depends on electron number and the location of the Mn^{2+} ion.

B. The effects of dot size and temperature

Nanostructures of semimagnetic semiconductor are expected to have higher Curie temperature of ferromagnetism than that of bulk materials.[12] The consequence is anticipated since the sp-d coupling in Eq. (4), known as the main cause of carrier-mediated ferromagnetism, is apparently enhanced if the size of semimagnetic nanostructures is reduced. Here, we can study the size effect by examining a representative case, the $N_e=3$ NC doped with Mn^{2+} at $\vec{R}_I=(0,0,a/2)$. In Fig. 6(a), we show the calculated magnetic susceptibility χ versus magnetic field B for NCs with $N_e=3$ and $a=3$, 4, 5, and 7 nm at $T=0.1$ meV. The feature of the magnetic susceptibility χ versus magnetic field B is found to be drastically changed with varying the size of the NC. For $a>5$ nm, the magnetic susceptibility decreases monotonically with increasing magnetic field. As the radius of NC is reduced to $a<5$ nm, a broad peak of magnetic susceptibility surprisingly emerges in low field. The χ peak arises from the GS transition in magnetic field of the $N_e=3$ Mn-doped NC, induced by the pronounced sp-d coupling in the small NCs. In the NC with $a<5$ nm, the strong coupling increases the critical field of the GS transition and the peak position shifts to higher field with decreasing the size of NC.

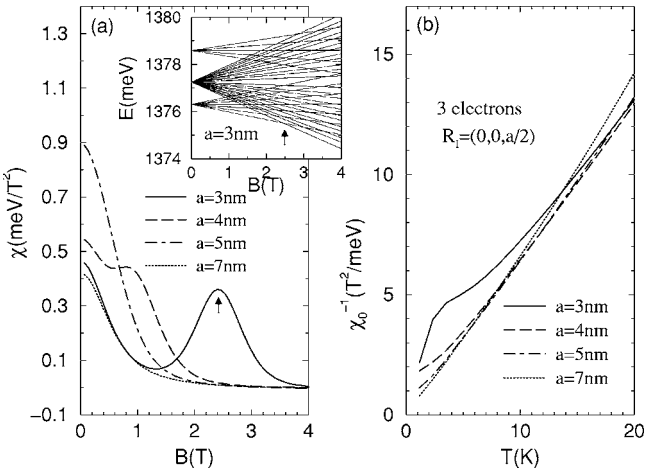

FIG. 6. (a) χ vs B and (b) χ_0^{-1} vs temperature T of the $N_e=3$ NCs with the Mn^{2+} ion located at $R_I=(0,0,a/2)$ and radius $a=3$, 4, 5, and 7 nm. Here we define $\chi_0\equiv\chi(B\rightarrow 0)$. The inset shows the energy spectrum vs B of the Mn-doped NC with $a=3$ nm. Arrows denote the critical magnetic field where GS transition occurs.

Figure 6(b) shows the calculated χ_0^{-1} versus T for the same NCs. For large NCs, the curves χ_0^{-1} versus T preserve the linearity, in agreement with the Curie law. However, as the NC size is down to $a<5$ nm, the linearity is broken at low temperature. For the NC with $a=3$ nm, a variation of the linearity appears at $T<10$ K. At low T, the low-field magnetic susceptibility is dominated and suppressed by the GS with $L_z=0$. As temperature is sufficiently high so that the thermal energy becomes comparable with the sp-d coupling, the excited states with finite angular momenta start to be involved in the magnetic response. It turns out that the suppression of the low-field magnetic susceptibility is released at the high T. Notable is that those signatures associated with the sp-d coupling in the magnetic response of nanostructures is pronounced only if the size of nanostructures is at the scale of few-nanometer, which is a typical scale for NCs but too small for SQDs.

IV. CONCLUSION

In summary, we have presented theoretical results on the magnetic properties of spherical nanocrystals containing

interacting electrons and a single spin-5/2 magnetic impurity. We found that the low-field paramagnetism, strongly depending on the number of electron and the location of Mn ion, is viewed as the manifestation of the GS properties of Mn-doped NCs. The competition between electron-electron interaction and the *sp-d* coupling between electron carriers and Mn ion leads to the pronounced anisotropy of magnetic properties, ground state transitions in magnetic field, and the violation of Hund's second rule. The *sp-d* coupling is significantly enhanced by the quantum confinement of NCs with radius of a few nanometers and leads to the violation of the Curie law at low temperature.

ACKNOWLEDGMENTS

The author acknowledges Pawel Hawrylak, Fanyao Qu, and Wen-Bing Jian for stimulating his interest in the subject and valuable discussions. The work was supported by National Science Council of Taiwan under Grant No. NSC-93-2112-M-009-020.

[1] S. C. Erwin, L. Zu, M. I. Haftel, A. L. Efros, T. A. Kennedy, and D. J. Norris, Nature (London) **436**, 91 (2005), and references therein.
[2] F. V. Mikulec, M. Kuno, M. Bennati, D. A. Hall, R. G. Griffin, and M. G. Bawendi, J. Am. Chem. Soc. **122**, 2532 (2000).
[3] D. J. Norris, N. Yao, F. T. Charnock, and T. A. Kennedy, Nano Lett. **1**, 3 (2001).
[4] T. Ji, W. B. Jian, and J. Fang, J. Am. Chem. Soc. **125**, 8448 (2003).
[5] L. Besombes, Y. Leger, L. Maingault, D. Ferrand, H. Mariette, and J. Cibert, Phys. Rev. Lett. **93**, 207403 (2004).
[6] L. Besombes, Y. Leger, L. Maingault, D. Ferrand, H. Mariette, and J. Cibert, Phys. Rev. B **71**, 161307(R) (2005).
[7] Al. L. Efros, M. Rosen, and E. I. Rashba, Phys. Rev. Lett. **87**, 206601 (2001).
[8] P. Recher, E. V. Sukhorukov, and D. Loss, Phys. Rev. Lett. **85**, 1962 (2000).
[9] J. K. Furdyna, J. Appl. Phys. **64**, R29 (1988).
[10] T. Dietl, Semicond. Sci. Technol. **17**, 377 (2002), and references therein.
[11] H. Saito, V. Zayets, S. Yamagata, and K. Ando, Phys. Rev. Lett. **90**, 207202 (2003).
[12] J. Fernandez-Rossier and L. Brey, Phys. Rev. Lett. **93**, 117201 (2004).
[13] D. M. Hoffman, B. K. Meyer, A. I. Ekimov, I. A. Merkulov, Al. L. Efros, M. Rosen, G. Couino, T. Gacoin, and J. P. Boilot, Solid State Commun. **114**, 547 (2000).
[14] P. S. Dorozhkin, A. V. Chernenko, V. D. Kulakovskii, A. S. Brichkin, A. A. Maksimov, H. Schoemig, G. Bacher, A. Forchel, S. Lee, M. Dobrowolska, and J. K. Furdyna, Phys. Rev. B **68**, 195313 (2003).
[15] A. A. Maksimov, G. Bacher, A. McDonald, V. D. Kulakovskii, A. Forchel, C. R. Becker, G. Landwehr, and L. Molenkamp, Phys. Rev. B **62**, R7767 (2000).
[16] A. K. Bhattacharjee and J. Perez-Conde, Phys. Rev. B **68**, 045303 (2003).
[17] A. O. Govorov, Phys. Rev. B **70**, 035321 (2004).
[18] N. Q. Huong and J. L. Birman, Phys. Rev. B **69**, 085321 (2004).
[19] J. Seufert, G. Bacher, M. Scheibner, A. Forchel, S. Lee, M. Dobrowolska, and J. K. Furdyna, Phys. Rev. Lett. **88**, 027402 (2002).
[20] A. M. Yakunin, A. Yu. Silov, P. M. Koenraad, J. H. Wolter, W. Van Roy, J. De Boeck, J.-M. Tang, and M. E. Flatte, Phys. Rev. Lett. **92**, 216806 (2004).
[21] U. Banin, Y. Cao, D. Katz, and O. Millo, Nature (London) **400**, 542 (1999).
[22] D. L. Klein, R. Roth, A. K. L. Lim, A. Paul Alivisatos, and P. L. McEuen, Nature (London) **389**, 699 (1997).
[23] B. Alperson, S. Cohen, I. Rubinstein, and G. Hodes, Phys. Rev. B **52**, R17017 (1995).
[24] D. Klein, P. L. McEuen, J. E. Bowen Katari, and A. P. Alivisatos, Appl. Phys. Lett. **68**, 2574 (1996).
[25] P. A. Maksym and T. Chakraborty, Phys. Rev. B **45**, R1947 (1992).
[26] L. G. G. V. Dias da Silva and M. A. M. de Aguiar, Phys. Rev. B **66**, 165309 (2002).
[27] I. Magnusdottir and V. Gudmundsson, Phys. Rev. B **61**, 10229 (2000).
[28] M. P. Schwarz, D. Grundler, M. Wilde, Ch. Heyn, and D. Heitmann, J. Appl. Phys. **91**, 6875 (2002).
[29] J. I. Climente, M. Korkusinski, P. Hawrylak, and J. Planelles, Phys. Rev. B **71**, 125321 (2005).
[30] F. Qu and P. Hawrylak, Phys. Rev. Lett. **95**, 217206 (2005).
[31] C. Gould, A. Slobodskyy, T. Slobodskyy, P. Grabs, D. Supp, P. Hawrylak, F. Qu, G. Schmidt, and L. W. Molenkamp, cond-mat/0501597 (unpublished).
[32] E. P. A. M. Bakkers, Z. Hens, A. Zunger, A. Franceschetti, L. P. Kouwenhoven, L. Gurevich, and D. Vanmaekelbergh, Nano Lett. **1**, 551 (2001).
[33] M. Shm, C. Wang, and P. Guyot-Sionnest, J. Phys. Chem. B **105**, 2369 (2001).
[34] Y. Z. Hu, M. Lindberg, and S. W. Koch, Phys. Rev. B **42**, 1713 (1990).
[35] A. K. Bhattacharjee and C. Benoit a la Guillaume, Phys. Rev. B **55**, 10613 (1997).
[36] P. Hawrylak, Phys. Rev. B **60**, 5597 (1999).
[37] S.-J. Cheng, W. Sheng, and P. Hawrylak, Phys. Rev. B **68**, 235330 (2003).
[38] See, e. g., S. Blundell, *Magnetism in Condensed Matter* (Oxford University Press, New York, 2001), Chap. 2.
[39] The magnetic susceptibility for a particle with angular momentum $J=I+S$ is proportional to $g_J^2 J(J+1)$ according to Eq. (5), where the Lande g-value $g_J=(g_I+g_S)/2+[(g_I-g_S)/2][I(I+1)-S(S+1)]/[J(J+1)]$ is associated with the g-factor values of the electron (g_S) and the Mn^{2+} ion (g_I). Considering a spin $S=1/2$ electron coupled to a single $I=5/2$ Mn^{2+} ion, the Lande g-value can be written as $g_J=g_I(x+5)/6$, where $x \equiv g_S/g_I$. Substituting the Lande g-value into Eq. (5), it is straightforward to show that the paramagnetism from the $J=3$ electron is higher than that from a system with decoupled $S=1/2$ electron and $I=5/2$ Mn if the x

value is in the range $4-\sqrt{15}<x<4+\sqrt{15}$. For CdSe:Mn NC, we have $x=0.6$ ($g_S=1.2$, $g_I=2.0$).

[40] Y. H. Zeng, B. Goodman, and R. A. Serota, Phys. Rev. B **47**, 15660 (1993).

[41] L. P. Levy, D. H. Reich, L. Pfeiffer, and K. West, Physica B **189**, 204 (1993).

[42] Y. Gefen, D. Braun, and G. Montambaux, Phys. Rev. Lett. **73**, 154 (1994).

[43] Hund's second rule states that, once the total spin is determined, the electrons in GS choose the largest value of total angular momentum whenever possible (Ref. 38). According to the rule, the p-shell electrons in the $N_e=3$ GS ($N_e=4$ spin-triplet GS) of spherical NCs are expected to have $|L_z|=1$ ($|L_z|=1$).